

Received February 8, 2021, accepted March 27, 2021, date of publication April 2, 2021, date of current version April 13, 2021.

Digital Object Identifier 10.1109/ACCESS.2021.3070533

Ranking Subassemblies of Wind Energy Conversion Systems Concerning Their Impact on the Overall Reliability

MOHAMED F. EL-NAGGAR^{1,2}, AHMED SAYED ABDELHAMID³, MOSTAFA A. ELSHAHED^{4,5},
AND MOHAMED EL-SHIMY MAHMOUD BEKHET⁶

¹Department of Electrical Engineering, College of Engineering, Prince Sattam Bin Abdulaziz University, Al-Kharj 16273, Saudi Arabia

²Department of Electrical Power and Machines Engineering, Faculty of Engineering, Helwan University, Helwan 11795, Egypt

³Electrical Power and Machines Department, Higher Institute of Engineering, El'Shorouk City 11837, Egypt

⁴Electrical Power Department, Faculty of Engineering, Cairo University, Giza 12613, Egypt

⁵Electrical Engineering Department, College of Engineering, Buraydah Private Colleges, Buraydah 51418, Saudi Arabia

⁶Electrical Power and Machines Department, Faculty of Engineering, Ain Shams University, Cairo 11566, Egypt

Corresponding authors: Mohamed F. El-Naggar (mfelnaggar@yahoo.com) and Ahmed Sayed Abdelhamid (eng_ahmed_sayed2010@yahoo.com)

ABSTRACT In this paper, an extensive reliability analysis of wind energy conversion systems (WECS) is presented. Elaborate the analysis is presented starting from the subassembly level to the subsystem level, then the system or the overall WECS. The fault tree method with a Weibull probability distribution function is introduced as a complete model for estimating the wind turbine subassemblies' reliability. The model was tested using a massive dataset of failure rates of various wind turbine subassemblies derived from relevant literature, comprising various operating concepts and the different climate conditions. In addition, ranking for various subassemblies of wind energy conversion systems concerning their impact on the overall system reliability is also presented in this paper to identify the weak items and subsystems. This identification guides the designers and planners in setting the appropriate maintenance strategies to increase the overall reliability of the considered systems and achieve a desired level of reliability. The results indicate that the model has practical applications for managing wind turbines, and the implementation demonstrates the proposed approach's effectiveness and efficiency, which may significantly enhance the WECS reliability.

INDEX TERMS Renewable energy, wind energy, reliability, fault tree analysis.

I. INTRODUCTION

Wind harvesting technologies represent the most essential and promising alternative sources of renewable power generation [1]. The wind farms have a high efficiency compared with photovoltaic power stations and tidal power and represent a green energy source compared with biomass and nuclear power plants. In past decades, the world has seen a rapid growth of the variable renewable systems-based installed capacities. For instance, the global installed capacity of wind turbine generators (WTGs) was only 6.1 GW in 1996, while this value reached 591 GW in 2018 with an annual growth rate lying between 10 and 40 percent [2]. By 2030, wind energy's global installed capacity is expected to attain about 2000 GW [3]. There is no doubt that wind energy

generation systems will play a significant role in the future energy mix [4].

Reliability and economics represent two inevitable and fundamental characteristics of wind energy power generation. Reliability refers to the system's ability to adequately perform its function under certain conditions for a given intended time. Simultaneously, economics represents an ultimate cost-benefit evaluation of a power system on an acceptable level of reliability. There is a direct relation between economics and reliability that has a very impact on investment decisions. Several factors may arise in power grids operation and management when connecting the electricity generated from wind energy systems with the grid. The first factor is related to the random and intermittence due to the uncertainty in wind speed. The second factor refers to the non-dispatchable energy, i.e., the electricity output is small compared to the volatility of distributed power. The third factor relates to

The associate editor coordinating the review of this manuscript and approving it for publication was Yu Wang.

the connection mode with the grid, where the power system's complexity will be increased due to the co-existence of on-grid and off-grid modes. The reliability of the power system will certainly be affected by these factors. Simultaneously, the initial investment cost, installment cost, and equipment replacement cost of the wind energy systems are substantially higher than the conventional fossil fuel-fired power generation. However, the installations of environment-dependent variable renewable energy (VRE) systems have been increased into the electrical grids to meet most countries' national strategic plans as a solution to reduce carbon emission, as stated before. Therefore, transmitting electricity uninterruptedly at a relatively lower cost represents one main goal of the modern power grid. Thus, the crucial characteristic of an electric power system that used more investigations is VRE systems' reliability [5].

Reliability represents the crucial issue in the planning and long-term operation of VRE systems. It helps predict system behavior over time only and is used for putting appropriate maintenance strategies accordingly, resulting in limits revenue losses [6]. However, the unavailability of accurate data of the subassemblies' failure and repair rates reduces the critical role of reliability in such systems. Therefore, a significant part of the existing literature has considered only one subsystem or even specific subassemblies only in reliability studies, such as the electrical subsystem [7], various types of the used generators [8], [9], or specific subassemblies [10]–[12]. Additionally, the data used was depending only on one location and one generating technology. The main reason behind the previous considerations is to avoid the unavailability of accurate reliability data for some subassemblies or even overcome the complexity arising from connected more than one subsystem.

On the other hand, a Reliability evaluation of the whole system has been conducted, in much fewer studies, using oversimplified assumptions that may lead to controversial observations between simulated and real results as stated in more details [13]. In this paper, an up-to-date dataset for failure rates of WECS subassemblies is presented to solve the problem of lacking accurate reliability data. The confidence of the results increases by collecting huge amounts of the subassemblies' failure and repair rates. Collecting huge amounts of failure rates of WECS subassemblies, which cover various large-scale system configurations and meteorological conditions, increased the results' confidence.

Researchers have used several reliability methods to evaluate the reliability of the WECS. Among them, reliability block diagram (RBD) and fault tree analysis (FTA) as seen in earlier reliability work [11], [14]–[16]. In FTA, a logical diagram is used to interpret the physical layout of the system. Each block in this logical diagram described only by the failure rate represents a system subassembly. The failure rate of each subassembly is used to determine the reliability of the whole WECS system. Thus, every failure rate is critical in the reliability study. Although failure rates are assumed constant in most reliability studies, more recent work has proven that

the failure rates must describe by time-dependent probability density functions (PDFs) with VRE systems [17].

The time-dependent PDF is valid for all periods of the subassembly's lifecycle and is used to model decreasing, increasing, and constant failure rates according to the bathtub curve. One of the most common time-dependent distributions used in reliability engineering and valid for all subassembly lifecycle periods is the Weibull distribution.

In this paper, a technique for evaluating the reliability of WECS is presented using the Weibull distribution-based fault tree analysis method [17]. The required input data are obtained from worldwide databases of various subassembly failures of WECS considering various operating concepts and the different climate conditions. This paper also aims to define the criticality of each subassembly of the WECS from the reliability point of view using the Fussel-Vesely method.

The rest of the paper is organized as follows. Section II shows the various layouts of the WECS, and Section III illustrates the various subassemblies of wind turbines. Section IV proposes the various configurations of wind turbines considered in this study. The reliability and maintenance of wind turbines are explained in Section V. System reliability modeling using fault tree analysis is presented in section VI. The simulation results are presented in Section VII. Section VIII, finally, provides the conclusions of this paper.

II. VARIOUS LAYOUTS OF WECS

The selection of an appropriate layout of WECS has a significant impact on achieving an acceptable reliability level of such systems. Still, it is also represented as an essential issue for reliability enhancement. There are two main layouts of WECS; grid-connected WECS and off-grid WECS. In the grid-connected system, the grid utility is directly fed from these systems, and the presence of a storage device is related to the level of grid reliability. If the degree of grid reliability was lower than the acceptable level, and the grid is insufficient for supplying local loads, storage devices would be necessary. At the same time, there is no need for storage devices with grid-connected systems if the grid's reliability level was more significant than or equal to the acceptable limit. In this case, the grid will secure supplying the local load by the power balance constraint and acts as energy storage with unlimited capacity.

According to the consequential impacts of power interruptions, the power system loads are classified into three categories; non-essential, essential, and critical loads. In the non-essential load type, long interruptions of power are allowed. Whereas very short interruptions of power are acceptable with the non-essential load type. In critical loads, the power interruptions are not acceptable for any reason and even very short durations. Consequently, when the grid-connected WECS used with the grid has a low-reliability level, the energy storage system is utilized for providing the power for essential and critical loads in the case of the grid outage. The overall system, in this case, thus, acts as the Uninterruptible Power Supply (UPS) [18]–[22].

On the other hand, when the traditional electricity sources (the utility grid) fail to deliver electricity to a distinct situation of the far loads, the off-grid systems will represent the appropriate choice to cover these loads. In this case, the load instantaneous power balance constraint will play an important role in the energy storage requirements with these systems. When deferrable loads that refer to a load type at which its energy requirements can be postponed to another nearby time are fed from off-grid WECS, the requirement of an energy storage system with the system is decreased. Storage tanks may be used for utilizing the surplus power for water storage in irrigation water pumping systems that represent the popular example of deferrable loads [23]. Unlike the deferrable loads, and for obtaining proper operation, an instantaneous power balance is required with the non-deferrable loads. Hence, the requirement of the energy storage system is increased with off-grid WECS that supply non-deferrable loads. According to the various operational modes and the load types, Figure 1 demonstrates the energy storage requirements for the WECS.

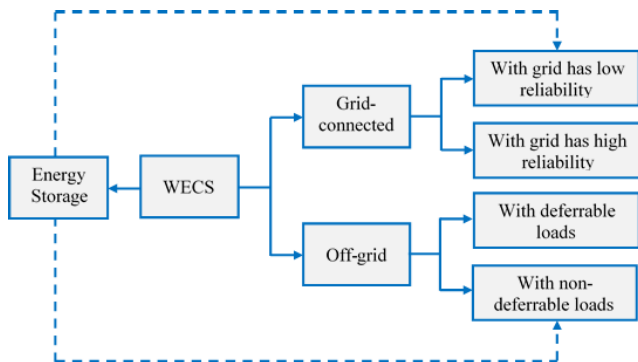


FIGURE 1. The requirements of energy storage for various layouts of the wind energy conversion system (WECS).

It is essential to point out that there are two options for energy storage systems. These options are the electrochemical storage system and non-electrical storage system. Several types of batteries are utilized with the electrochemical energy storage system. In contrast, the second option (the non-electrical energy storage) can be provided with many options such as pumped storage, hydrogen, and compressed air energy storage (CAES). Various options of energy storage have been discussed in detail in [24].

Driven by the above discussions about the various layouts of WECS, Figure 2 and Figure 3 illustrate the layouts' details considering the electrochemical storage system. The DC-DC converter (CON) acts as a Maximum Power Point Tracker (MPPT) in layouts without electrical energy storage. At the same time, it also acts as a charge controller in layouts with battery storage. The Static Automatic Transfer Switch (SATS) is used with the grid-connected WECS that feeds the non-reliable grid to provide the immediate islanding WECS through its sensing and switching control logic. The grid is disconnected in the island mode due to either an outage or a severe power quality problem. As a result, the non-essential

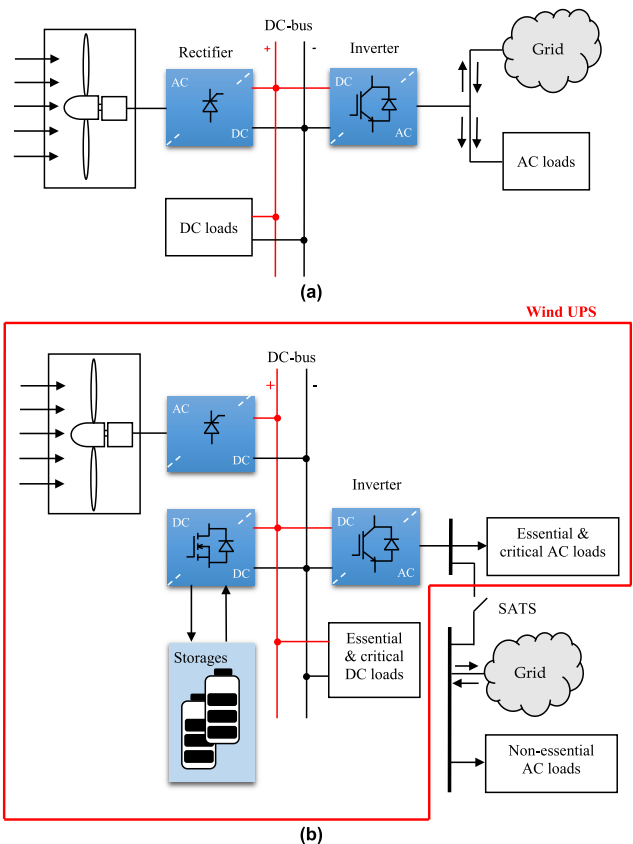


FIGURE 2. Various layouts of grid-connected WECS with (a) the grid has sufficient high-reliability level; (b) the grid has a low-reliability level.

loads are isolated from the WECS, which provides only the required energy for the essential and critical loads. In the island mode, the power balance is secured by battery energy storage.

Generally, the reliability of the renewable power plants depends on the reliability of the primary resource, outside the variable renewable energy (VRE) system, and/or the reliability of each subassembly in the system. Therefore, two trends are taken in order to assess the reliability of the renewable systems in reliability studies; reliability assessment of the system vulnerable subassemblies and reliability evaluation of the whole system considering the variable resources. This paper is related only to the first trend that studies the reliability of the system's vulnerable subassemblies [25].

III. VARIOUS SUBASSEMBLIES OF WIND TURBINES

The numbers of subassemblies vary according to the type and size of WT. The main subassemblies of a typical wind turbine are illustrated in Figure 4. As shown in Figure 4, the mechanical energy is transmitted by blades connected to the hub via a low-speed shaft to the gearbox's high-speed shaft. The main bearing is used to support the low-speed shaft, while the gearbox is used to adjust speed. The converter is utilized in some wind turbines to match the grid connection. The yaw system is mounted on a bedplate or foundation at

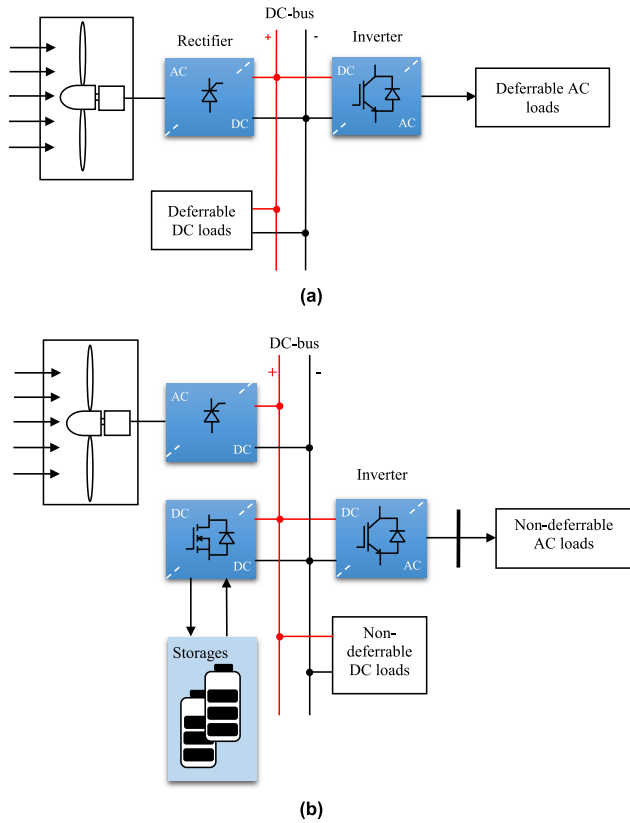


FIGURE 3. Various layouts for off-grid WECS with (a) deferrable loads; (b) non-deferrable loads.

the top of a tower. It is used to rotate the nacelle to control the alignment of the direction of the wind. The pitch system mounted in each blade acted as an aerodynamic brake and is used to control the amount of power going to the wind turbine. The yaw, the brake, and the pitch system are controlled by a meteorological unit attached to provide weather data (e.g., wind speed and direction).

According to the wind turbines’ types and sizes, the costs of all of these subassemblies will vary. For instance, some wind turbines do not have a gearbox at all in some configurations. Therefore, depending on the configuration used, the costs of both generators and converters will differ. Anyway, Figure 5 illustrates the distribution of the costs of the subassemblies for a typical 2 MW wind turbine [13].

The whole wind turbine generation system is decomposed into three subsystems according to their function. These subsystems are electrical, mechanical, and other subsystems. Each subsystem is then divided into subassemblies. Furthermore, according to each subassembly’s severity in the case of failure on energy production from the wind system, another classification of wind turbine subassemblies is considered. Generally, the function of the wind turbine system may be classified into three states as “operational state,” “failed state,” and “degraded operation state.” During the operational state, the wind turbine operates at full capacity and produces its expected electricity because its subassemblies

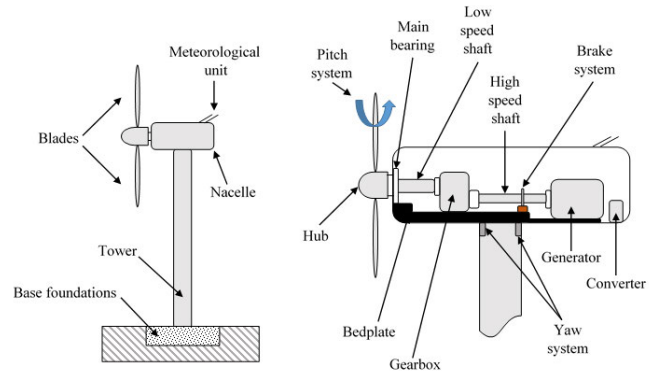


FIGURE 4. Wind turbine subassemblies.

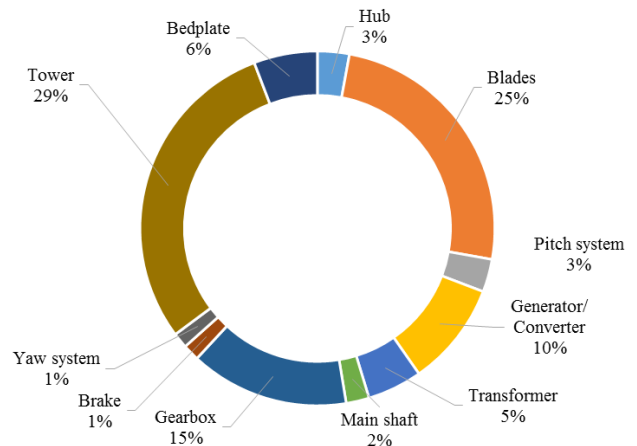


FIGURE 5. Distribution of the costs of the subassemblies for a typical 2 MW wind turbine.

can work properly. During the failed state, the wind turbine cannot operate because the wind turbine subassemblies have a failure, and this failure will directly affect the wind turbine performance. The operational and failed states are called binary states. These states are traditional states that are discussed during modeling the wind turbine system as a whole. The third state of degraded operation is introduced by [7].

During this state, the wind turbine system is performing its function with an efficiency lesser. From this explanation of the wind turbine system’s function, the wind turbine subassemblies can be classified into two main categories as primary subassemblies and secondary subassemblies. Any failure in the primary subassemblies may lead to taking the wind turbine from the operational state to the failed state. In contrast, any secondary subassemblies’ failure may change the wind turbine from the operation state to the degraded operation state. The wind turbine subassemblies shown in Figure 4 are classified according to their function into electrical subassemblies, mechanical subassemblies, and other subassemblies and according to their severity into primary and secondary subassemblies as recorded in Table 1. The function of each subassembly is also stated. Secondary subassemblies are considered as minor contributors to global

TABLE 1. Wind turbines subassemblies.

Subsystems	Subassemblies	Functionality	Subassembly type
Electrical subsystem	Generator (GN)	Converts mechanical energy into electrical energy	Primary
	Converter (CN)	Converts AC signal into a DC signal	Primary
	Electrical parts (EP)	Connects the WT with the grid	Primary
Mechanical subsystem	Gearbox (GB)	Converts the rotational speed from low value into high value	Primary
	Yaw System (YS)	Turns the WT into the wind direction	Primary
	Blades (BL)	Captures the wind energy and converts it into mechanical energy	Primary
	Pitch system (PS)	Controls blades to increase or decrease the speed of WT	Primary
	Mechanical brake (MB)	Locks the WT if the wind speed is high	Secondary
	Air brake (AB)	Controls the tip blades to decrease the speed of WT and helps to look it	Secondary
	Main Shaft (MS)	Transmits the mechanical energy from the gearbox to the generator	Primary
	Hydraulic system (HS)	Controls some subsystems of the WT (e.g., Yaw sys, Mech. Br, Air Br)	Secondary
Other subsystems	Anemometer (AN)	Measures wind speed	Secondary
	Sensors (SE)	Indicates the state of some subassemblies	Secondary
	Hub (HU)	Turns the low-speed shaft inside the WT with blades connected to it	Primary
	Tower (TW)	Protects the inner subassemblies of the WT from external factors	Primary

system reliability but can't be ignored [7]. However, it is essential to point out that the secondary subassemblies will significantly contribute to the global system reliability if the root causes of the secondary subassemblies are extended to any of the primary subassemblies [15].

IV. VARIOUS CONFIGURATIONS OF WIND TURBINES CONSIDERED IN THIS STUDY

In the last few decades, various configurations of wind turbines with innovative technology have been developed to increase the output power. The horizontal axis, three blades, and the wind turbine are considered the most common configuration. Various combinations of rotational speed, drive train configuration, generator, and power control can be used in this typical configuration.

Constant or variable rotational speed can be obtained. For the narrow range of rotational speed, the former only can be utilized. The mechanical stresses being lower, and the energy of the wind being extracted more efficient in the case of power electronic converters for adapting the output to the grid frequency [26].

There are three categories of power control; passive stall, active stall, or pitch system. In the passive stall system, the angles of blades are fixed to the hub. In strong winds, the blades are designed to stall. However, in the active stall system, the blade's angle is easily adjustable to create a stall and blades. Still, it doesn't increase the captured wind energy in large wind turbines, where the increasing need for braking in emergency cases, stall control has been considered unfeasible [26].

The blades can turn about their longitudinal axis in the pitch system to optimize the captured wind energy. A Pitch system in which the blades can turn about their longitudinal axis has been considered an excellent system to optimize the captured wind energy. Additionally, it will also act as a brake on the rotor in undesirable weather conditions. Of course, the electrical or hydraulic mechanisms in the blades will increase the cost of the wind turbine.

According to the gearbox's presence or no, the wind turbines are classified into two main categories; indirect-drive or direct-drive systems. In the first system (indirect-drive), the gearbox increases the rotational speed of the main (high speed) shaft that drives the generator. The direct-drive system doesn't include the gearbox but uses different generators and electric power converter to adapt the energy to the grid frequency.

There are main types of generators used in wind turbines, such as doubly-fed induction generator (DFIG), wound rotor induction generator (WRIG), squirrel-cage induction generator (SCIG), electrically excited synchronous generator (EESG), and permanent magnet synchronous generator (PMSG) [27]. Indirect-drive configurations use lower and less expensive than direct-drive types.

Stall control with constant speed machines has taken under pitch control and the variable speed machines. Synchronous generators seem to be replaced by the DFIG. DFIG based wind turbines are considered as the most type offered by the major manufacturers. This study will focus only on two configurations (Type I and Type II) of the wind turbines from the configuration point of view.

Type I: variable speed wind turbines with partial-scale frequency converter:

DFIG is used in this type of wind turbine, in which the stator of the WRIG is directly connected to the grid, and a partial-scale power frequency converter is connected to the rotor circuit. This configuration usually uses a multi-stage gearbox. The rotor speed range relates to the size of the used power frequency converter, and a more excellent band range of speeds can be obtained when using larger converters. The range of the variable speed is typically around $\pm 30\%$ of the synchronous speed. The maximum efficiency that can be obtained in this system is around 70%. The partial-scale power converter will take around 25% and 30% of the generator's nominal output power. Due to the reactive power compensation realized through a converter, the capacitor bank is not required.

Type II: variable speed direct-drive wind turbines with full-scale frequency converter:

In these wind turbines, the variable speed is adjusted by the pitch control system, and a full-scale frequency converter is used to connect the generator with the grid utility. This configuration of wind turbines characterizes by a gearless drive train. A Full-scale power converter used with multi-pole generators represents the main reason behind not using the gearbox. Two groups fall under this configuration according to the type of generator used. The first group uses an electrically excited synchronous generator (EESG), while the second group has a permanent magnet synchronous generator (PMSG). In this situation, there is an increasing need for a more massive generator with a larger number of poles because this configuration has a low rotor speed. Direct drive types commanded approximately 17.4% of the global WT market in 2010, which is expected to be 24.3% by 2016 [13].

V. RELIABILITY AND MAINTENANCE OF WIND TURBINES

There is an increasing need for complicated maintenance systems, due to the high machinery cost and infrastructure of wind turbines stated above in addition to the difficulty of access to them by maintenance personnel; if high reliability, availability, maintainability, and safety (RAMS) [14] are to be achieved. Of course, this will reflect on the cost of failure. For bearing failure as an example, the cost of repairing this failure or even refurbishment of the faulty item could be 5000 € in the case of detecting the failure. In comparison, this value could rise to more than 250.000 € if not detecting the failure due to collateral damage to other subassemblies [28]. Consequently, it is essential to point out that selecting the best maintenance systems represents the first step towards cost reduction.

As a result of employing the condition monitoring (CM) incorporated with the supervisory control and data acquisition (SCADA) systems, a significant improvement has been recorded in the field of wind turbine maintenance and repair strategies. The usage of CM, fault detection and diagnosis (FDD), and fault detection algorithms consider as an early warning for mechanical, structural, and electrical defects, enabling the operators in the wind farms to carry out predictive maintenance and hence reducing failure rates [29]. Smaller wind turbines require less preventive maintenance than larger ones [30]. In tandem with predictive maintenance, preventive maintenance is usually used. Both of them are very important for offshore wind turbines where the maintenance personnel operates at the weather's mercy.

Using the CM system, faults can be predicted with reasonable accuracy 60 min before they occur [31]. Figure 6 demonstrates the P-F curve in which the deterioration failure leading up to the fault is illustrated. The potential fault at point P is possibly detected. The deterioration continues until functional failure at point F if the failure is not mitigated. The fault can be avoided through the time between P and F [13]. Due to high wear, of course, some subassemblies have

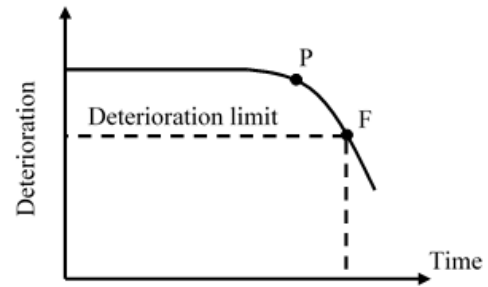


FIGURE 6. P-F curve.

higher failure rates than others. These subassemblies are rotor blades, gearboxes, and generators.

A. BASICS CONCEPTS AND MATHEMATICS OF RELIABILITY

The cumulative failure distribution (CDF), denoted $Q(T)$, is the distribution used to represent time-dependent values of the probability of failure, and it is also called failure probability. This function is also defined as the probability of un-surviving in a given time, t . Thus, it is also known as unreliability or un-survivor function. This function increases from zero to one as the random variable increases from its smallest to its most massive value. The increase appears in continuous steps for discrete random variables and continuously for continuous random variables.

The reliability or the survivor function denoted $R(t)$ is used to evaluate the “non-probability of failure” in a given time. It is defined as the probability of a system, subsystem, or even subassembly to perform its required function adequately, under the given operating conditions, for an intended period. It is also defined as the probability of surviving, successfully operating the system within a given time, t . So, the survivor function is a complementary value of the cumulative failure distribution $Q(t)$, and it can be expressed as:

$$R(t) = 1 - Q(t) \quad (1)$$

The probability density function (PDF), denoted $f(t)$, is defined as the failure distribution over the entire time range. Therefore, it is the derivative of the cumulative distribution function of continuous random variables. Thus, it can be written as:

$$f(t) = \frac{dQ(t)}{dt} = -\frac{dR(t)}{dt} \quad (2)$$

Then, the cumulative failure distribution function and the reliability function can be written with a function of the density function as:

$$Q(t) = \int_0^t f(t) dt \quad (3)$$

$$R(t) = \int_t^{\infty} f(t) dt \quad (4)$$

Failure density function, reliability function, and cumulative failure distribution function are demonstrated in Figure 7, considering exponential distribution function with failure rate $\lambda = 0.2$. It is denoted that the total area under the failure density function is equal to the summation values of unreliability $Q(t)$ and reliability $R(t)$. The regions that describe the values of $Q(t)$ and $R(t)$ also illustrated in Figure 7.

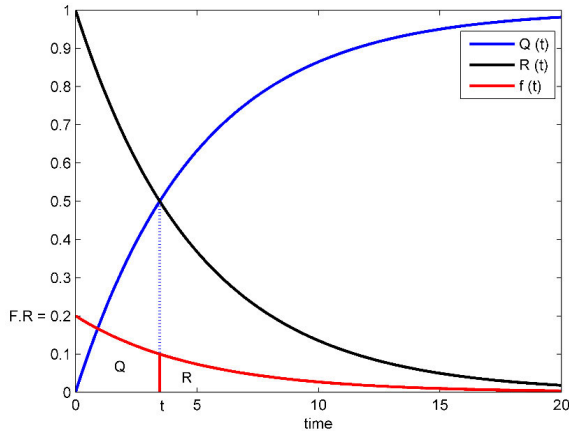


FIGURE 7. Unreliability function $Q(t)$, reliability function $R(t)$, and failure density function $f(t)$ considering exponential distribution function with $\lambda = 0.2$.

Hazard function or transition rate function refers to the number of transitions that a subassembly makes between one state and another. It may be associated with failure (failure rate), repair (repair rate), or any other relevant transition. In general, it is designed as $\lambda(t)$, where:

$$\lambda(t) = \frac{f(t)}{R(t)} \tag{5}$$

A typical relationship between failure rate and time, known as the bath-tub curve, is shown in Figure 8. Failures of wind turbines are commonly assumed to follow a bath-tub curve [32]. The typical lifetime of the new wind turbine is around 20 years. It is illustrated from the bath-tub curve that the total lifetime of any subassembly breaks into three distinct periods. The first period, in which the rates of failure are high then decreases, is the period of early failures. It is noted that the rates of failure seem to be constant by lower rates in the second period that known as the period of the useful lifetime [33]. In the third period, known as the wear-out period, the failure rates are increased with time. Tavner *et al.* [32] presented data from German turbines operating in their early failure periods and Danish ones in their periods of use. They failed to find any data for wear-out periods because the WTs were relatively new and because WTs that lose reliability tend to be taken out of service before wear out. Periods of early failure appear to be getting longer [34]. From the reliability point of view, the reliability and availability of various power system subassemblies are executed in the second period (useful life). The exponential probability density function is valid [7].

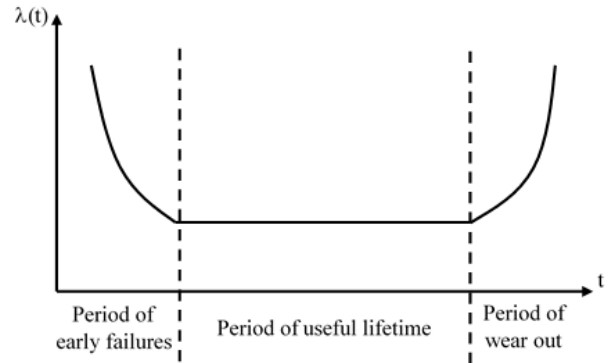


FIGURE 8. Distribution of failures over the life cycle of the wind turbine (bath-tub curve).

The relationship between $R(t)$ and $\lambda(t)$ for all distributions can exist as follows:

$$f(t) = \lambda(t) \times R(t) \tag{6}$$

From Equation (2) and Equation (5), we get:

$$-\frac{dR(t)}{dt} = \lambda(t) \times R(t) \tag{7}$$

Then,

$$\frac{1}{R(t)} dR(t) = -\lambda(t) dt \tag{8}$$

By integrating both sides of equation (8), we get:

$$\int_{R(0)}^{R(t)} \frac{1}{R(t)} dR(t) = \int_0^t -\lambda(t) dt \tag{9}$$

$$\therefore \ln(R(t)) \Big|_{R(0)}^{R(t)} = \int_0^t -\lambda(t) dt \tag{10}$$

$$\therefore \ln(R(t)) = \int_0^t -\lambda(t) dt \tag{11}$$

Thus,

$$R(t) = e^{\left(\int_0^t -\lambda(t) dt\right)} \tag{12}$$

Equation (12) is the general equation of the reliability function as a function of the hazard function, and it's valid with all distributions. In a particular case, when the failure rate is constant and independent with time, as in the period of the useful lifetime in the bath-tub curve, the reliability is given by the following equation.

$$R(t) = e^{-\lambda t} \tag{13}$$

This particular case, which is known as the exponential distribution, interprets that the reliability in the period of the useful lifetime obeys the exponential distribution function or the exponential distribution function is valid only in

the second period of the bath-tub curve. The duration of the useful lifetime is very dependent on the subassembly being used. The mechanical subassemblies a short useful lifetime, while the electronic subassemblies have a long useful life. Many power system subassemblies are made to remain within their useful life period by constant and careful preventive maintenance [7].

One of the most common distributions used in reliability engineering is the Weibull distribution, which plays a critical role in the statistical analysis of failure rate data. It has no characteristic shape, and the selection of values for its parameters makes it extremely flexible, where various shapes attain through different values of the shape parameter β . The Weibull distribution can be used to model decreasing, increasing, and constant failure rates that enable it to model various data and life characteristics. The 2-parameter Weibull probability density function is given by:

$$f(t) = \frac{\beta}{\eta} \times \left(\frac{t}{\eta}\right)^{\beta-1} \times e^{-\left(\frac{t}{\eta}\right)^\beta} \quad (14)$$

where:

$$\begin{aligned} f(t) &\geq 0 \\ t &\geq 0 \\ \beta &> 0 \\ \eta &> 0 \end{aligned}$$

The Weibull reliability function is given by:

$$R(t) = e^{-\left(\frac{t}{\eta}\right)^\beta} \quad (15)$$

The Weibull failure rate function is given by:

$$\lambda(t) = \frac{\beta}{\eta} \times \left(\frac{t}{\eta}\right)^{\beta-1} \quad (16)$$

- The failure rate decreases with time, if $0 < \beta < 1$.
- The distribution becomes the exponential distribution, the particular case, and the failure rate is constant when $\beta = 1$.
- The Weibull assumes wear-out type shapes, i.e., the failure rate increases with time when $\beta > 1$.

B. RELIABILITY DATA PREPARATION

Collecting accurate reliability data is considered the main challenge in reliability assessment. The recorded reliability data in some wind farms are not available, and the retrieval of these data is too expensive. Even if field reliability data were available, these usually don't satisfy the selected model's assumptions for analysis. Furthermore, the data used depended only on one site and one technology, and not considering the period of the collected data specified as a short period in more cases. Besides, the traditional studies for the reliability of the wind energy conversion systems focus only on the reliability analysis of these systems throughout analyzing only one subsystem or even considering the large subassemblies for conducting reliability assessment.

A considerable amount of reliability data for all subassemblies comprising the system is collected from various locations with different climatic conditions, various operating technologies, and different operation duration periods to overcome the previous disadvantages. Table 2 lists the failure rate for various subassemblies of WECS. This paper suggests a novel framework, shown in Figure 9, to determine the wind turbine subassemblies' Weibull parameters using subassemblies failure rate. The results of the simulation are shown in Table 3. The probability density distributions for MTBF of various wind turbine subassemblies of DFIG and DDSG are shown in Figure 10. It is clear that from Figure 10 that the converter records the higher failure probability among all electrical subassemblies in DFIG.

In comparison, the electrical parts record the higher failure probability among all electrical subassemblies in DDSG. For the mechanical subsystem, pitch system and air brake represent the highest failure probability for DFIG and DDSG, respectively. For DDSG, the hub represents the higher failure probability among all subassemblies. For DFIG, hub represents the higher failure probability among all subassemblies after excepting (pitch system). Some researchers have concluded that the electrical subassemblies are the leading cause of lost days per year [3], [11]. Some other researchers have found that mechanical failure recorded around 79% of failures in wind turbines [9].

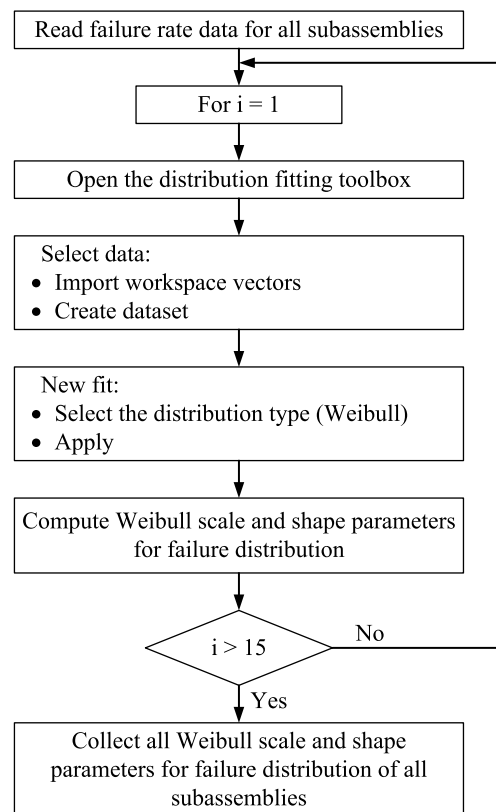


FIGURE 9. Framework for estimating the Weibull parameters for all subassemblies of WECS.

TABLE 2. Failure rate for various subassemblies of WECS.

Subassembly	References															
	DFIG								DDSG							
	[15]	[10]	[37]	[37]	[38]	[39]	[40], [41]	[42]	[13]	[8]	[43]	[38]	[38]	[10]	[43]	[43]
GN	0.22	0.12	0.11	0.15	0.27	0.08	0.02	0.35	0.35	0.13	0.30	0.35	0.12	0.08	0.30	0.35
CN	0.56	0.11	0.01	0.07	0.36	0.10	0.07	0.30	0.31	0.31	0.31	0.32	0.29	0.59	1.27	1.11
EP	NA	NA	0.01	0.01	NA	0.11	0.05	0.58	0.54	0.50	0.53	NA	NA	NA	1.46	1.38
GB	NA	NA	0.13	0.18	0.55	0.15	0.05	Missing in this technology								
YS	NA	NA	0.01	0.01	0.16	0.10	0.03	0.12	0.11	0.17	0.11	0.12	0.14	NA	0.24	0.19
BL	NA	NA	0.12	0.17	0.21	0.20	0.05	0.25	0.24	0.14	0.24	0.24	0.17	NA	0.32	0.24
PS	NA	NA	0.01	0.01	0.50	NA	NA	0.30	0.30	0.47	0.29	0.29	0.42	NA	NA	NA
MB	NA	NA	0.01	0.01	NA	0.04	0.01	0.06	NA	0.02	0.01	NA	NA	NA	0.03	0.03
AB	Missing in this technology								NA	NA	NA	0.19	NA	NA	NA	NA
MS	NA	NA	0.05	0.04	NA	NA	0.01	0.09	0.08	0.05	0.07	NA	NA	NA	NA	NA
HS	NA	NA	NA	NA	NA	0.36	0.06	NA	0.02	NA	NA	NA	NA	NA	NA	NA
AN	NA	NA	NA	NA	NA	NA	NA	0.09	0.08	0.07	0.09	NA	NA	NA	NA	NA
SE	NA	NA	NA	NA	NA	0.12	0.05	0.12	0.12	0.26	0.15	NA	NA	NA	0.51	0.49
HU	NA	NA	0.12	0.14	NA	0.01	0.01	NA	NA	NA	NA	NA	NA	NA	0.56	0.51
TW	NA	NA	0.15	0.14	NA	0.09	0.01	NA	NA	NA	NA	NA	NA	NA	0.38	0.27

NA: Not available

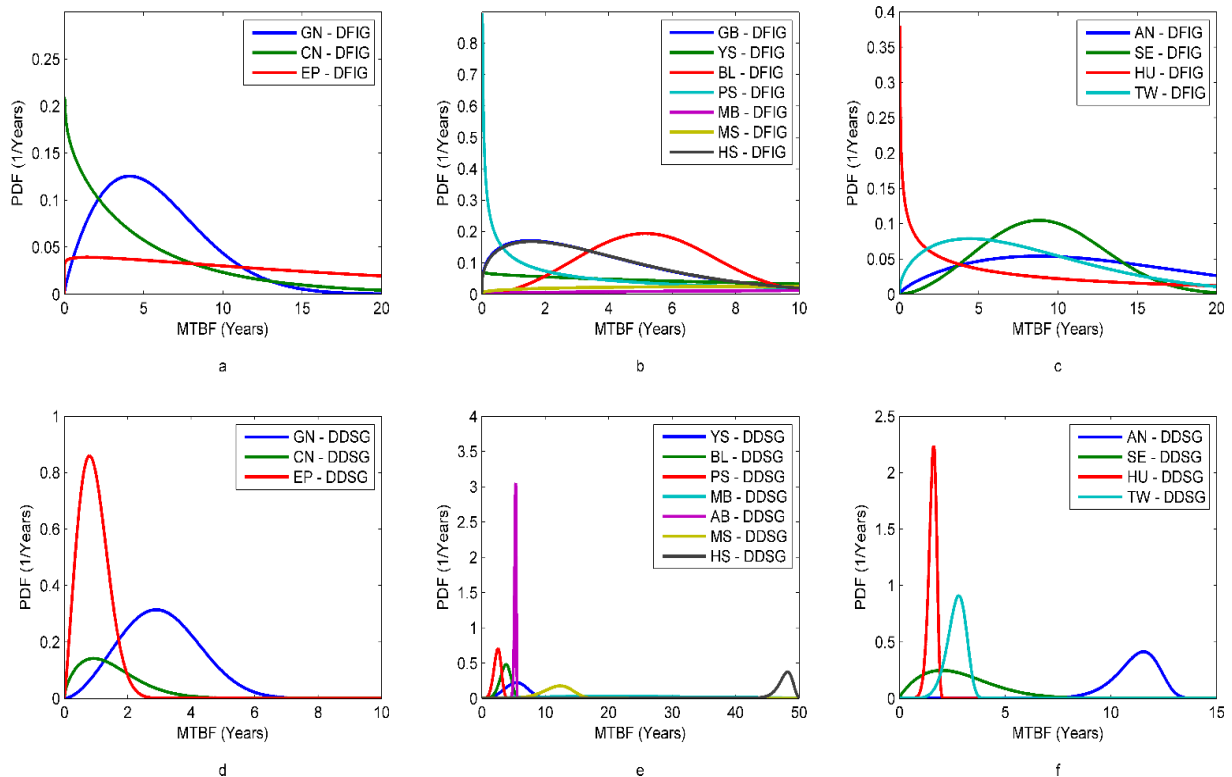


FIGURE 10. Probability Density Function (PDF) for MTBF of various wind turbine subassemblies of DFIG and DDSG.

These findings were also supported partially by our previous work [11], seeing that some systems fall within the median range of the subassemblies' failure rates. However,

they are not expected to pose any downtime problems to wind turbines, whereas other systems fall within the high range of the subassemblies' failure rates that will lead to

TABLE 3. Estimated Weibull parameters of WECS subassemblies.

Subassembly	Weibull PDF parameters of subassemblies failure rate			
	DFIG		DDSG	
	η	β	η	β
GN	6.43	1.81	3.43	2.71
CN	5.32	0.94	1.66	1.63
EP	21.70	1.06	1.06	2.17
GB	4.30	1.33	M	M
YS	16.34	0.97	6.03	3.53
BL	5.94	2.93	4.00	5.12
PS	10.23	0.54	2.67	4.98
MB	50.88	1.51	29.42	1.91
AB	M	M	5.34	44.38
MS	29.81	1.30	12.75	6.06
HS	4.37	1.34	48.21	49.18
AN	14.55	1.71	11.61	13.02
SE	10.40	2.74	3.21	1.77
HU	18.97	0.65	1.64	9.89
TW	9.44	1.48	2.87	7.02

M: Missing in this technology

stopping the wind turbine, as was inferred by these authors. Figure 11 shows the subassemblies of failure rates per year of DFIG and DDSG. By substituting the scale and shape parameters listed in Table 3 into Equation (15), the percentage of reliability of each subassembly of the studied WECS for one year and ten years of operations were estimated (see Table 4). As shown in Table 4, after ten years of operation, a quick decline in reliability is noted. For instance, after one year of operation, the generator had a 96.60% probability of operating without failures, while after ten years of operation, it had only a 10.84% probability. Reliability of 0% means that at least one subassembly of the WECS is failed and does not mean that the overall system is failed.

It is essential to point out that the data represent the first and important stage that ensures the success of using the proposed framework. Thus, it is crucial to existing a validation stage

TABLE 4. Subassemblies reliability [in %].

Subassembly	% R			
	DFIG		DDSG	
	After one year	After ten years	After one year	After ten years
GN	96.60	10.84	96.51	0.000
CN	81.11	16.43	64.41	0.000
EP	96.24	64.40	41.14	0.000
GB	86.60	4.63	M	M
YS	93.60	53.77	99.82	0.003
BL	99.46	1.01	99.92	0.000
PS	75.25	37.23	99.24	0.000
MB	99.73	91.73	99.85	0.881
AB	M	M	96.02	0
MS	98.79	78.51	100.00	0.795
HS	87.04	4.82	100.00	1
AN	98.98	59.06	100.00	0.867
SE	99.84	40.70	88.13	0.001
HU	86.13	51.62	99.23	0.000
TW	96.47	33.64	99.94	0.000

M: Missing in this technology



FIGURE 11. Subassemblies failure rate per year.

before using the data if they are not sufficient. The validation stage may compare the data used with the field data for a system with the same operation condition and performance.

VI. SYSTEM RELIABILITY MODELLING USING FAULT TREE ANALYSIS

Reliability modeling represents a critical stage in the reliability evaluation of WECS. Researchers in reliability studies have utilized various reliability modeling techniques to evaluate the reliability of such systems. Among them, a reliability block diagram (RBD) and fault tree analysis (FTA). The RBD method's system subassemblies are represented by either parallel or sequential blocks that describe the failure and repair rates of these subassemblies. The interconnections between the blocks are dependent on the effect of each block on the whole system. RBD method is preferable when satisfying failure and repair rates are available to perform complete reliability, availability, and maintainability (RAM) analysis. On the other hand, FTA is a graphical design method in which failures are defined more easily than non-failures. In this method, the physical layout is interpreted into a logical diagram whereby each block represents a system subassembly, and the failure rate is used for describing each block.

For analyzing the risk and reliability of causal systems, FTA represents the most useful tool. It is a graphical design method used when failures are defined more easily than non-failures. In this method, the focus is usually on a failure appearing at the top of the fault tree diagram. The prediction of most system failures in a system breakdown represents one of the significant advantages of FTA. The link of failure processes of logic diagrams, which show the system's state and behavior, is attempted by FTA. The top event defines the system's failure mode, or its function analyzed in terms of its subassemblies' failure modes and influence factors. Gates are used to assigning the fault tree. These gates are present the relationships between their input and output events. More details about fault tree techniques can be found in [35].

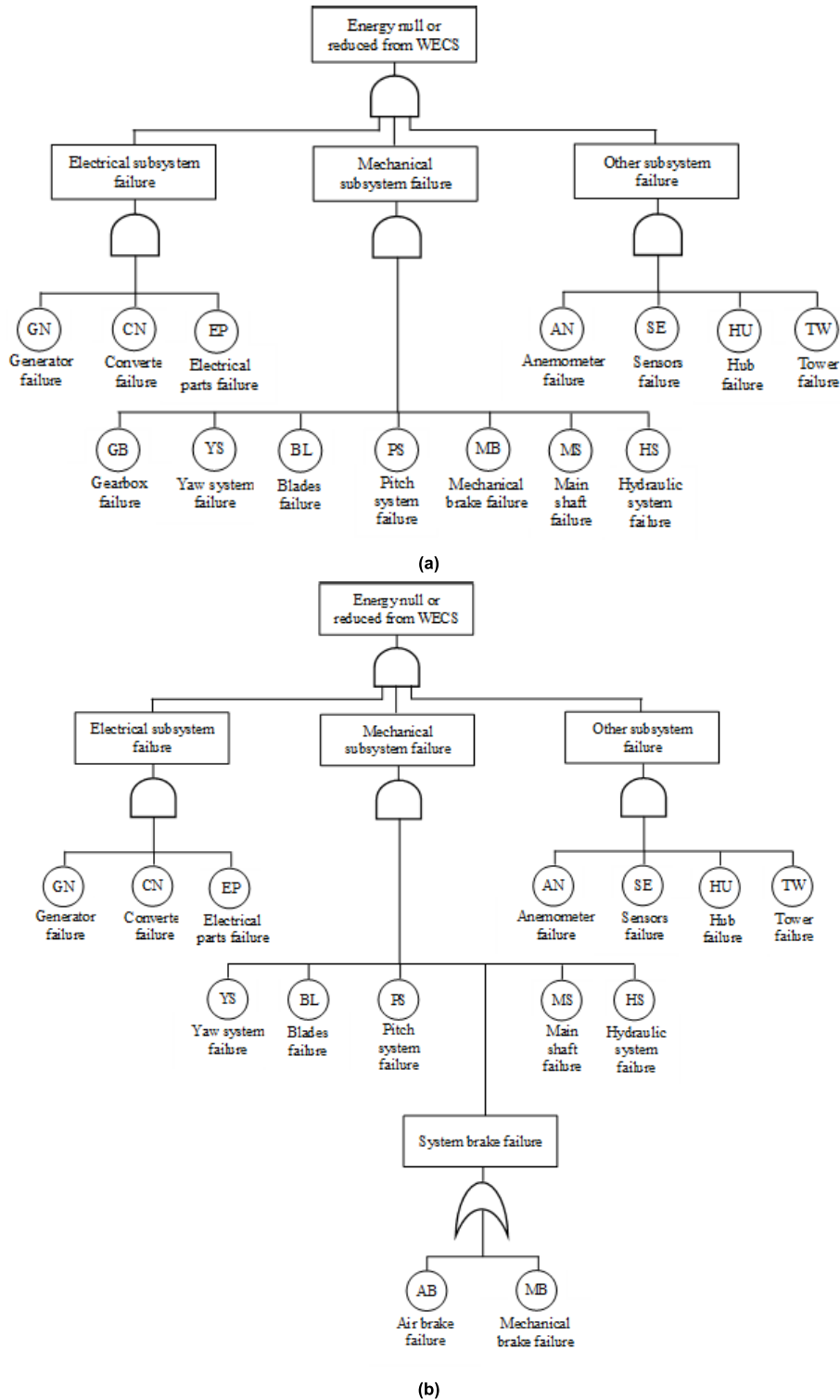


FIGURE 12. Fault tree of the WECS (a) DFIG; (b) DDSG.

In the present work, the reliability of WECS is obtained utilizing the system approach model based on logic gate (fault tree) representation. Logic diagrams are used to model the pre-described systems mathematically and express their reliability. The system may contain only series subassemblies, parallel subassemblies, or a combination of both. These

configurations help in understanding the logic relationship. The reliability of a series of subassemblies can be computed by Equation (17) as in [36].

$$R_s(t) = \prod_{i=1}^K [R_i(t)], \quad i = 1, \dots, n \quad (17)$$

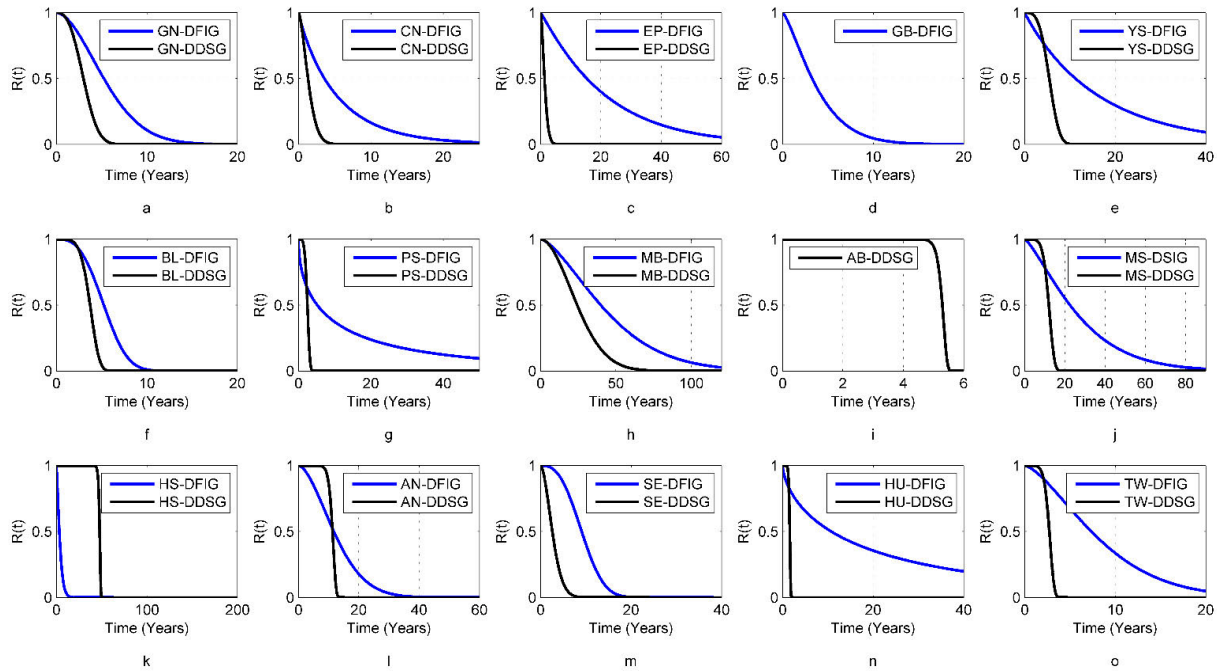


FIGURE 13. a: Survivability trend of the generator. b: Survivability trend of the converter. c: Survivability trend of electrical parts. d: Survivability trend of the gearbox. e: Survivability trend of the yaw system. f: Survivability trend of blades. g: Survivability trend of pitch system. h: Survivability trend of a mechanical brake. i: Survivability trend of air brake. j: Survivability trend of the main shaft. k: Survivability trend of the hydraulic system. l: Survivability trend of the anemometer. m: Survivability trend of sensors. n: Survivability trend of the hub. o: Survivability trend of the tower.

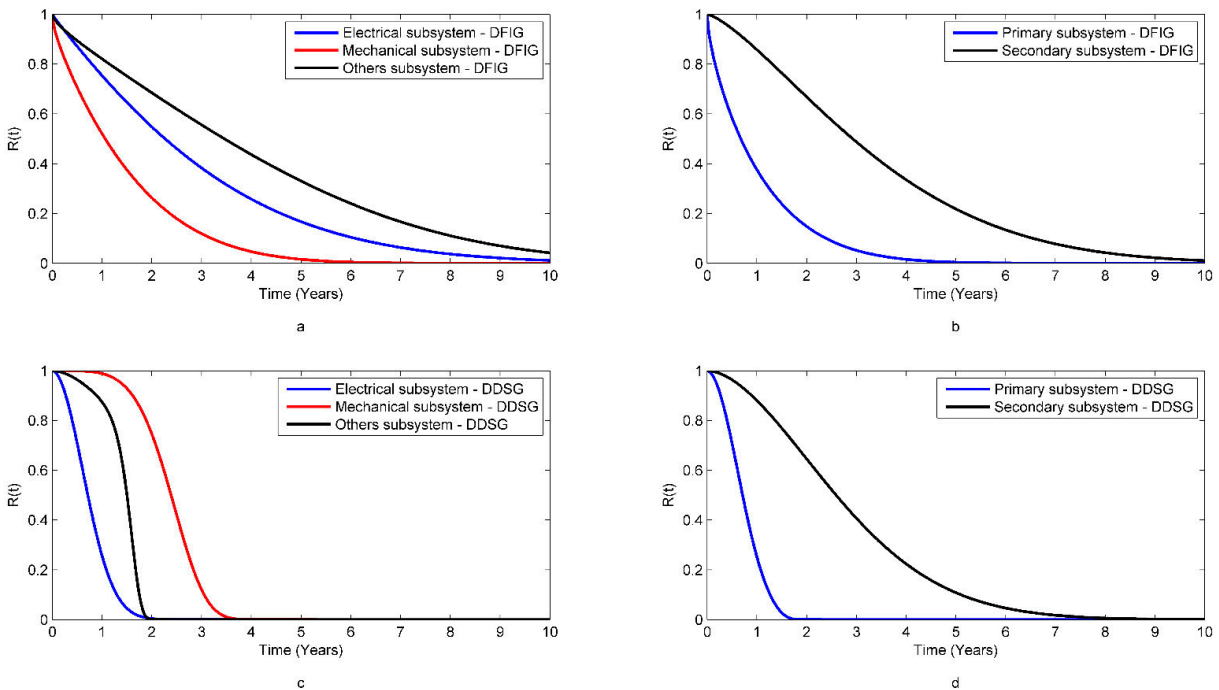


FIGURE 14. Survivability trend for various subsystems of WECS.

where $R_i(t)$ is the reliability of the system/subassemblies [36]. Further, the reliability of the parallel subassemblies is computed as:

$$R_p(t) = 1 - \prod_{i=1}^K [1 - R_i(t)], \quad i = 1, \dots, n \quad (18)$$

Figure 12 shows a fault tree for the considered wind energy conversion systems in this paper. As shown in Figure 12, the system may have more than one top event. The box that appears on the top event represents the failure event under investigation. For instance, Energy null or reduced from the WECS was determined as a top

event in this study. The following basic symbols represent the relationship between the top event and lower events:

- AND gate: if all combinations of the events shown below the gate (the input events) exist, the event above the gate will occur.
- OR gate: if at least one combination of the events shown below the gate (the input events) exist, the event above the gate will occur.
- Rectangle: The rectangle, the main block of FTA, represents an adverse event. It is located at the top of the tree or throughout the tree to denote other interest events.

VII. SIMULATION AND RESULTS

The survivability of the wind turbine subassemblies studied in this work is shown in Figure 13(a)-13(o). It is evident from these figures that all subassemblies of the DFIG configuration have a long lifecycle duration and higher reliability than the subassemblies of the DDSG configuration. Due to several issues such as that manufacturing defects, installation problems, material characteristics, and environmental concerns, random failures can occur at any time in the lifecycle of a subassembly [44], [45]. However, subassemblies that have lower lifecycle durations’ limits require more frequent inspection than others due to their high proneness to failure. These subassemblies are the generator, gearbox, and blades in DFIG configuration and the most DDSG configuration subassemblies. Therefore, these subassemblies must be monitored more often than others since they may contribute more to the wind turbine’s downtime. The main reason behind that the gearbox was reported as a non-reliable subassembly by many authors in literature [46]–[48], and the gearbox reliability issue can be mitigated through the application of necessary condition monitoring approaches. Furthermore, the DDSG requires a robust maintenance system to keep this configuration’s reliability above the desired limit. Figure 14 displays the survivability of the wind turbine subsystems studied in this work.

A modified Fussel-Vesely method is introduced in this work to obtain useful information. The effect of a single subassembly on the overall reliability of the system can be calculated as:

$$FV = 1 - e^{-\left(\frac{t}{\eta}\right)^\beta} \tag{19}$$

The Fussel-Vesely method reveals the impact of the generator, converter, electrical parts, gearbox, yaw system, blades, pitch system, brakes, main shaft, hydraulic system, anemometer, sensors, hub, and tower on the overall reliability of WECS. The Fussel-Vesely results after one year and ten years of operation are listed in Table 5. The ranking of the most critical subassemblies appears in Table 6.

TABLE 5. Results of fussel-vesely after one year and after ten years of operation.

Subassembly	FV			
	DFIG		DDSG	
	After one year	After ten years	After one year	After ten years
GN	3.40	89.16	3.49	100
CN	18.90	83.57	35.59	100
EP	3.76	35.60	58.86	100
GB	13.40	95.37	M	M
YS	6.40	46.23	0.18	99.74
BL	0.54	98.99	0.08	100
PS	24.75	62.77	0.76	100
MB	0.27	8.27	0.15	11.92
AB	M	M	3.98	100
MS	1.21	21.49	1.97e-5	20.47
HS	12.96	95.18	0	0
AN	1.02	40.94	1.35e-12	13.31
SE	0.16	59.30	11.78	99.94
HU	13.87	48.38	0.77	100
TW	3.53	66.36	0.06	100

M: Missing in this technology

TABLE 6. Critical subassembly priorities.

Subassembly	Priority	
	DFIG	DDSG
GN	04	01
CN	05	01
EP	12	01
GB	02	M
YS	10	02
BL	01	01
PS	07	01
MB	14	06
AB	M	01
MS	13	04
HS	03	07
AN	11	05
SE	08	03
HU	09	01
TW	06	01

M: Missing in this technology

VIII. CONCLUSION

In this study, a complete framework for evaluating the reliability of WECS has been carried out based on the Weibull probability distribution and fault tree analysis method. The ranking of the most critical subassemblies has been determined by utilizing the Fussel-Vesely method. Although a high rate of reliability of WECS could be obtained under frequent maintenance, however frequent maintenance is not an optimal solution. Maintenance strategies can be optimized to reduce the associated costs. Thus, the results of the Fussel-Vesely method are significant to indicate what priority of the subassemblies that the planned maintenance should focus on. This will contribute to select the appropriate maintenance strategies, which the future work will focus on, for all subassemblies of wind energy conversion system that, of course, will help for improving the overall system reliability. The

proposed method may be used with any other wind power systems considering the failure information used as an input stage of the proposed method. It's essential to point out that the input data should be collected carefully, over an appropriate time span, trusted, and obtained accurate results for helping the operators and developers implement appropriate maintenance strategies to enhance overall system reliability.

REFERENCES

- [1] R. Moeini, M. Entezami, M. Ratkovac, P. Tricoli, H. Hemida, R. Hoefler, and C. Baniotopoulos, "Perspectives on condition monitoring techniques of wind turbines," *Wind Eng.*, vol. 43, no. 5, pp. 539–555, Oct. 2019.
- [2] P. Zhou, R. Y. Jin, and L. W. Fan, "Reliability and economic evaluation of power system with renewables: A review," *Renew. Sustain. Energy Rev.*, vol. 58, pp. 537–547, May 2016.
- [3] *Renewables 2020 Global Status Report*, REN21, Paris, France, 2020.
- [4] K. Chaïmarit and S. Nuchprayoon, "Modeling of renewable energy resources for generation reliability evaluation," *Renew. Sustain. Energy Rev.*, vol. 26, pp. 34–41, Oct. 2013.
- [5] L. Goel, "Power system reliability cost/benefit assessment and application in perspective," *Comput. Electr. Eng.*, vol. 24, no. 5, pp. 315–324, Sep. 1998.
- [6] Y. F. Li, S. Valla, and E. Zio, "Reliability assessment of generic geared wind turbines by GTST-MLD model and Monte Carlo simulation," *Renew. Energy*, vol. 83, pp. 222–233, Nov. 2015.
- [7] R. Billinton and R. N. Allan, "System reliability evaluation using probability distributions," in *Reliability Evaluation of Engineering Systems*. Boston, MA, USA: Springer US, 1983, pp. 170–205.
- [8] P. Tavner and F. Spinato, "Reliability of different wind turbine concepts with relevance to offshore application," in *Proc. Eur. Wind Energy Conf.*, Brussels, Belgium, Mar./Apr. 2008.
- [9] G. M. J. Herbert, S. Iniyar, and R. Goic, "Performance, reliability and failure analysis of wind farm in a developing country," *Renew. Energy*, vol. 35, no. 12, pp. 2739–2751, Dec. 2010.
- [10] J. Carroll, A. McDonald, and D. Mcmillan, "Reliability comparison of wind turbines with DFIG and PMG drive trains," *IEEE Trans. Energy Convers.*, vol. 30, no. 2, pp. 663–670, Jun. 2015.
- [11] M. El-Metwally, M. El-Shimy, A. Mohamed, M. Elshahed, and A. Sayed, "Reliability assessment of wind turbine operating concepts using reliability block diagrams (RBDs)," in *Proc. 19th Int. Middle East Power Syst. Conf. (MEPCON)*, Dec. 2017, pp. 430–436.
- [12] S. Faulstich, B. Hahn, and P. J. Tavner, "Wind turbine downtime and its importance for offshore deployment," *Wind Energy*, vol. 14, pp. 327–337, Apr. 2011.
- [13] J. M. P. Pérez, F. P. G. Márquez, A. Tobias, and M. Papaelias, "Wind turbine reliability analysis," *Renew. Sustain. Energy Rev.*, vol. 23, pp. 463–472, Jul. 2013.
- [14] F. P. G. Márquez, J. M. P. Pérez, M. Papaelias, and R. R. Hermosa, "Wind turbines maintenance management based on FTA and BDD," *Renew. Energy Power Qual.*, vol. 3, pp. 1344–1346, Apr. 2012.
- [15] H. Arabian-Hoseynabadi, H. Oraee, and P. J. Tavner, "Wind turbine productivity considering electrical subassembly reliability," *Renew. Energy*, vol. 35, no. 1, pp. 190–197, Jan. 2010.
- [16] M. El-Metwally, M. EL-Shimy, M. Elshahed, and A. Sayed, "Detailed analyses of the failure and repair rates of wind and solar-PV systems for RAM assessment," *Int. Conf. Electr. Eng.*, vol. 11, no. 11, pp. 1–16, Apr. 2018.
- [17] F. Chiacchio, F. Famoso, D. D'Urso, S. Brusca, J. A. Unanue, and L. Cedola, "Dynamic performance evaluation of photovoltaic power plant by stochastic hybrid fault tree automaton model," *Energies*, vol. 11, p. 306, Feb. 2018.
- [18] D. P. Kaundinya, P. Balachandra, and N. H. Ravindranath, "Grid-connected versus stand-alone energy systems for decentralized power—A review of literature," *Renew. Sustain. Energy Rev.*, vol. 13, no. 8, pp. 2041–2050, Oct. 2009.
- [19] D. J. T. Siyambalapatiya, S. T. K. Rajapakse, S. J. S. de Mel, S. I. T. Fernando, and B. L. P. P. Perera, "Evaluation of grid connected rural electrification projects in developing countries," *IEEE Trans. Power Syst.*, vol. 6, no. 1, pp. 332–338, Oct. 1991.
- [20] M. Sidrach-de-Cardona and L. M. López, "Evaluation of a grid-connected photovoltaic system in southern Spain," *Renew. Energy*, vol. 15, nos. 1–4, pp. 527–530, Sep. 1998.
- [21] U. Atikol, "Impact of cogeneration on integrated resource planning of turkey," *Energy*, vol. 28, no. 12, pp. 1259–1277, Oct. 2003.
- [22] A. Fernández-Infantes, J. Contreras, and J. L. Bernal-Agustín, "Design of grid connected PV systems considering electrical, economical and environmental aspects: A practical case," *Renew. Energy*, vol. 31, no. 13, pp. 2042–2062, Oct. 2006.
- [23] A. Sayed, M. El-Shimy, M. El-Metwally, and M. ElShahed, "Overview for practical layouts of solar-PV and wind energy conversion systems," Aug. 2019, ch. 1, pp. 19–36.
- [24] A. Chatzivasileiadi, E. Ampatzis, and I. Knight, "Characteristics of electrical energy storage technologies and their applications in buildings," *Renew. Sustain. Energy Rev.*, vol. 25, pp. 814–830, Sep. 2013.
- [25] M. El-Shimy, "Alternative configurations for induction-generator based geared wind turbine systems for reliability and availability improvement," in *Proc. Mepcon*, 2010, pp. 538–543.
- [26] A. D. Hansen, F. Iov, F. Blaabjerg, and L. H. Hansen, "Review of contemporary wind turbine concepts and their market penetration," *Wind Eng.*, vol. 28, no. 3, pp. 247–263, May 2004.
- [27] H. Polinder, D.-J. Bang, H. Li, Z. Chen, M. Mueller, and A. McDonald, "Concept report on generator topologies, mechanical & electromagnetic optimization," *Optimization*, vol. 6, p. 79, Oct. 2007.
- [28] D. Mcmillan and G. W. Ault, "Condition monitoring benefit for onshore wind turbines: Sensitivity to operational parameters," *IET Renew. Power Gener.*, vol. 2, no. 1, pp. 60–72, Mar. 2008.
- [29] F. P. García Márquez, A. M. Tobias, J. M. Pinar Pérez, and M. Papaelias, "Condition monitoring of wind turbines: Techniques and methods," *Renew. Energy*, vol. 46, pp. 169–178, Oct. 2012.
- [30] B. Lu, Y. Li, X. Wu, and Z. Yang, "A review of recent advances in wind turbine condition monitoring and fault diagnosis," in *Proc. IEEE Power Electron. Mach. Wind Appl.*, Jun. 2009, pp. 1–7.
- [31] A. Kusiak and W. Li, "The prediction and diagnosis of wind turbine faults," *Renew. Energy*, vol. 36, no. 1, pp. 16–23, Jan. 2011.
- [32] P. J. Tavner, J. Xiang, and F. Spinato, "Reliability analysis for wind turbines," *Wind Energy*, vol. 10, no. 1, pp. 1–18, Jan. 2007.
- [33] G. Klutke, P. C. Kiessler, and M. A. Wortman, "A critical look at the bathtub curve," *IEEE Trans. Rel.*, vol. 52, no. 1, pp. 125–129, Mar. 2003.
- [34] E. Echavarría, B. Hahn, G. J. W. van Bussel, and T. Tomiyama, "Reliability of wind turbine technology through time," *J. Sol. Energy Eng.*, vol. 130, no. 3, Aug. 2008.
- [35] A. Ahadi, N. Ghadimi, and D. Mirabbasi, "Reliability assessment for components of large scale photovoltaic systems," *J. Power Sources*, vol. 264, pp. 211–219, Oct. 2014.
- [36] N. Gupta, R. Garg, and P. Kumar, "Sensitivity and reliability models of a PV system connected to grid," *Renew. Sustain. Energy Rev.*, vol. 69, pp. 188–196, Mar. 2017.
- [37] M. Shafiee and F. Dinmohammadi, "An FMEA-based risk assessment approach for wind turbine systems: A comparative study of onshore and offshore," *Energies*, vol. 7, no. 2, pp. 619–642, Feb. 2014.
- [38] H. Arabian-Hoseynabadi, P. J. Tavner, and H. Oraee, "Reliability comparison of direct-drive and geared-drive wind turbine concepts," *Wind Energy*, vol. 13, no. 1, pp. 62–73, Jan. 2010.
- [39] S. Mani and H. Oraee, "An availability evaluation approach for DFIG wind turbines considering subcomponents reliability," in *Proc. 2nd Iranian Wind Energy Conf.*, Tehran, Iran, 2014, doi: 10.13140/2.1.1386.9442.
- [40] J. Ribrant and L. M. Bertling, "Survey of failures in wind power systems with focus on Swedish wind power plants during 1997–2005," *IEEE Trans. Energy Convers.*, vol. 22, no. 1, pp. 167–173, Mar. 2007.
- [41] A. Ghaedi, A. Abbaspour, M. Fotuhi-Firuzabad, M. Moeini-Aghtaie, and M. Othman, "Reliability evaluation of a composite power system containing wind and solar generation," in *Proc. IEEE 7th Int. Power Eng. Optim. Conf. (PEOCO)*, Jun. 2013, pp. 483–488.
- [42] D. Topi, D. Šljivac, and M. Stojkov, "Reliability model of different wind power plant configuration using sequential Monte Carlo simulation," *Eksploatacja Niezawodnoscale Maintenance Rel.*, vol. 18, pp. 237–244, Mar. 2016.
- [43] E. Koutoulakos, "Wind turbine reliability characteristics and offshore availability assessment," M.S. thesis, TU Delft, Delft, The Netherlands, 2010.
- [44] *Implementation and Review of a Nuclear Power Plant Ageing Management Programme*, International Atomic Energy Agency, Vienna, Austria, 1999.
- [45] *Management of Life Cycle and Ageing at Nuclear Power Plants: Improved I&C Maintenance*, International Atomic Energy Agency, Vienna, Austria, 2004.

- [46] K. Kim, G. Parthasarathy, O. Uluyol, W. Foslien, S. Sheng, and P. Fleming, "Use of SCADA data for failure detection in wind turbines," *Energy Sustainability*, vol. 54686, pp. 2071–2079, Oct. 2011.
- [47] J. Igba, K. Alemzadeh, I. Anyanwu-Ebo, P. Gibbons, and J. Friis, "A systems approach towards reliability-centred maintenance (RCM) of wind turbines," *Procedia Comput. Sci.*, vol. 16, pp. 814–823, Dec. 2013.
- [48] W. Musial, S. Butterfield, and B. McNiff, "Improving wind turbine gearbox reliability," in *Proc. Eur. Wind Energy Conf.*, 2007, pp. 1–13.



MOHAMED F. EL-NAGGAR received the B.Sc., M.Sc., and Ph.D. degrees in electrical engineering from Helwan University, Egypt, in 1995, 2002, and 2009, respectively. He was with the Department of Electrical Power and Machines Engineering, Faculty of Engineering, Helwan University, from 1995 to 2013. Since 2013, he has been an Assistant Professor with the Department of Electrical Engineering, College of Engineering, Prince Sattam Bin Abdulaziz University, Saudi Arabia. His main

research interests include power system protection and switchgears, power transformers operation, testing, renewable energy, smart grids, and artificial intelligence.



AHMED SAYED ABDELHAMID was born in Cairo, Egypt, in 1986. He received the B.Sc. degree from the Higher Institute of Engineering, El'Shorouk Academy, in 2008, the M.Sc. degree from the Arab Academy for Science Technology and Maritime Transport (AASTMT), in 2015, and the Ph.D. degree from Cairo University, in 2019, all in electric power engineering. He is currently a Lecturer of the electrical power systems with the Department of Electrical Power and Machines,

Higher Institute of Engineering, El'Shorouk Academy. His research interests include electric power systems: analysis, stability, economics, optimization, distribution, renewable energy integration, transformers, power electronics, and reliability.



MOSTAFA A. ELSHAHED received the B.Sc., M.Sc., and Ph.D. degrees in electric power engineering from Cairo University, in 2005, 2008, and 2013, respectively. He was a Postdoctoral Researcher with the University of Porto, Portugal, and The University of Manchester, U.K. He is currently an Associate Professor with the Buraydah Private College and on leave from Cairo University. His research interests include power quality, power systems stability, power systems operations, stochastic optimization, and integration of renewable energy sources.



MOHAMED EL-SHIMY MAHMOUD BEKHET is currently a Professor of the electrical power systems with the Department of Electrical Power and Machines, Faculty of Engineering, Ain Shams University. He is also an Electromechanical Specialist, a Freelance Trainer, a Technical Advisor, and a member of many associations and professional networks. He is a Technical Reviewer with some major journals and conferences. His research interests include electric power systems: analysis, stability, economics, optimization, distribution, renewable energy integration, and reliability. For more information, please visit: <http://shimymb.tripod.com>.

...